NJC

Accepted Manuscript

This is an *Accepted Manuscript*, which has been through the Royal Society of Chemistry peer review process and has been accepted for publication.

Accepted Manuscripts are published online shortly after acceptance, before technical editing, formatting and proof reading. Using this free service, authors can make their results available to the community, in citable form, before we publish the edited article. We will replace this *Accepted Manuscript* with the edited and formatted *Advance Article* as soon as it is available.

You can find more information about *Accepted Manuscripts* in the Information for Authors.

Please note that technical editing may introduce minor changes to the text and/or graphics, which may alter content. The journal's standard Terms & Conditions and the Ethical guidelines still apply. In no event shall the Royal Society of Chemistry be held responsible for any errors or omissions in this *Accepted Manuscript* or any consequences arising from the use of any information it contains.

ROYAL SOCIETY OF CHEMISTRY

www.rsc.org/njc

Cite this: DOI: 10.1039/c0xx00000x

www.rsc.org/xxxxxx

ARTICLE TYPE

Fast and Continuous Processing of a new Sub- Micronic Lanthanide-based Metal-Organic Framework

Loïc D'Arras[a,b,c], Capucine Sassoye*[a,b,c], Laurence Rozes[a,b,c], Clément Sanchez[a,b,c], Jérôme Marrot[d], Samuel Marre[e], Cyril Aymonier*[e]

Received (in XXX, XXX) Xth XXXXXXXXX 20XX, Accepted Xth XXXXXXXXX 20XX
DOI: 10.1039/b000000x

Processing strategies for the synthesis of hybrid materials stands as a relevant way to modulate particles size and morphology. We present herein the use of a continuous high temperature / high pressure (HT/HP) process for the synthesis of a new cerium based metal organic framework (MOF). The HT/HP harsh thermodynamic synthesis conditions lead to MOF nanostructures exhibiting the same phase as for microparticles obtained through conventional batch solvothermal conditions but in exceptional much shorter residence times, opening avenues towards production scaling-up. HT/HP process also tailors down the size of the particles, which still present a major issue for most MOF applications.

1. Introduction

An extraordinary amount of research has appeared over the last decades in the field of hybrid materials, and more specifically in coordination polymers such as the metal organic framework family (MOF), indicating the growing interest of chemists, physicists, and materials researchers to fully exploit the opportunity of creating innovative materials and devices.[1, 2]

MOFs are hybrid crystalline compounds presenting great tunability: each original material is the result of the enlightened combined choice of metallic precursor and organic polyfunctionnal ligands[3] leading, under appropriate experimental conditions, to an extremely vast number of compounds with different structures and properties. These materials generally display regular nanoporosity (micro and / or meso) and reach very high specific surface (S_{BET} as high as 6000 m²/g),[4] leading to a great accessibility of the metallic centers. Most of the materials published so far exhibits divalent or trivalent metals[5-8] or lanthanides[9]. This leads to a wide range of properties among which gas separation or storage[10, 11] and catalysis have been widely explored to take advantage of the great accessibility to the metallic centers.[12-14] The cavity confinement effect has been proven to be highly effective on polymerization,[15, 16] optics,[17] drug delivery[18, 19] or sensoring.[20] Despite the superior properties that can be expected, much fewer compounds have been published with high oxidation number metals as the metallic precursor's reactivity is generally much higher and makes these elements difficult to handle. However, several compounds with tetravalent metals[21, 22] have been characterized and used in catalysis, for instance in CO_2 reduction applications.[23] Another aspect concerns the size of the obtained MOF particles, mostly in the micrometer range,[24] whereas smaller nanostructured particles could bring additional advantages in most of these applications.

Several synthesis strategies have been considered in the literature, the most common methods remaining hydrothermal or solvothermal syntheses in batch mode. Nevertheless, other methods were recently proposed to enhance crystallization and reduce particles' size using microwaves[25, 26] or ultrasounds[27], mechanical grinding[28-30] These have been shown to be relevant ways to get nanostructures, which can be later packed to reach homogeneous coatings using process like dip-coating.[31] All these approaches are appropriate for studying the fundamental properties of MOF, however, they generally require long residence times and tend to suffer from irreproducibility of size, size distribution, and quality of the materials from batch to batch. It is also difficult to implement fast screening and optimization of the synthesis conditions in batch, and there are challenges in scaling batch procedures up to quantities needed for development and optimization. Oppositely, HT/HP continuous flow reactors integrated with fluid control elements, offer a solution to these challenges, as well as additional advantages, including feedback control of temperature, pressure and feed streams, reproducibility, fast mixing of reagents and rapid screening of parameters. These processes enable reactions to be performed under specific conditions - such as supercritical conditions -[32-35] with higher yields than can typically be achieved with conventional batch reactors, which could become important for the synthesis of novel materials. In particular, kinetics can be drastically modified and lead to extremely short synthesis times, as recently reported by Lester *et al.* to reproduce and modify the size of the versatile well-known copper terephthalate HKUST-1[36]. From this initial demonstration, one can envision using such processes to access new MOFs structures with tunable size down to the nanoscale.

As evidence that new MOFs synthesis processes - especially continuous ones allowing implementing easy scale-up of nanostructured materials - are of increasing interest, a spray-drying strategy has been recently used for the synthesis of nanoscale metal–organic frameworks hollow superstructures.[37, 38] Different applications can be considered through a relevant choice of the metal ion used for MOFs' synthesis. In particular,

lanthanides ions are commonly used in these materials, mainly for their luminescent properties.[39] They display large ionic radius and large coordination spheres (up to 12),[40] therefore a potentially great number of extension points, leading to structural richness. Solvent molecules are often needed to complete the coordination sphere in addition to the carboxylate ligands. These solvent molecules are quite labile. Their departure creates, *in situ*, unsaturated metallic centers,[41, 42] which is a considerable advantage for catalysis. A shortcoming of this lability is the structure weakening and therefore a relative difficulty to obtain stable materials.

Cerium is one of the biggest cation in the lanthanide family[43] and exhibits two main oxidation states. Diamagnetic Ce(IV) stands as a strong oxidant and is widely used in catalysis.[44, 45] It reacts very fast with many organic compounds,[46] leading to Ce(III) materials. Paramagnetic Ce(III) leads to compounds with unique magnetic[47, 48] and luminescent characteristics,[49, 50] which can be used for the synthesis of materials displaying magnetically ordering[51] or scintillation properties.[52] Given this large scope of properties, cerium-based MOFs stand as high potential materials.

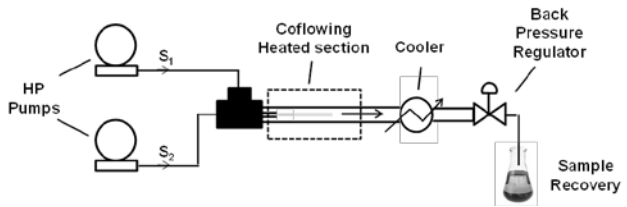

Fig. 1: HT-HP coflow reactor for the continuous synthesis of MOFs, including high pressure pumps, oil bath, cooler and back pressure regulator.

In this paper, we demonstrate the use of a high-throughput continuous HT/HP process to synthesize nanostructures of a new cerium(III)-terephthalate Metal-Organic Frameworks exhibiting an original topology. This new synthesis approach was compared with conventional batch solvothermal synthesis.

2. Experimental Section

2.1 Materials and Methods

Chemicals were analytical reagent grade purchased from Sigma-Aldrich and used as received without any further purification step.

TEM and SEM snapshots were acquired from aTecnai spirit G2and a Hitachi S-3400Nmicroscope, respectively, allowing observation of the Cerium-based MOF micro- and nanostructures. Powder diffraction patterns were obtained from a Bruker D8 instrument equipped with a cupper anode ($<\lambda(K_{\alpha1}, K_{\alpha2})>$= 1.5418Å)

Thermodiffraction analyses were performed with a X'Pert Pro Panalytical and an Anton Paar HTK 1200N oven, under air, also equipped with a cupper anode.

TGA experiments were carried on a Netzsch STA 409 device. XPS spectra were collected on a SPECS GmbH X-Ray Photoelectron spectrometer using a Mg Kα (hm = 1253.6 eV) monochromatedradiation source having a 300 W electron beam power. Kinectic energies were measured by a hemispheric analyser (Phoibos 100 -5 Mutiple Channel Detector).

2.2 Synthesis

HT/HP synthesis*:* the experiments were carried out in a coaxial flowing microsystem made of two stainless steel capillaries (inner diameters: $\varnothing_1$ = 0.5 mm, $\varnothing_2$ = 2.1 mm, length = 1 m) as shown in Figure 1. Heating was provided by an oil bath (T = 230 °C), whereas the pressure was controlled with a back-pressure regulator downstream (P = 10MPa). The precursor solution constituted of ammonium cerium (IV) nitrate (CAN, $Ce(NH_4)_2(NO_3)_6$, 0.045 M) and terephthalic acid (0.09 M) in DMF is injected in the inner stainless steel tubing (flow rate = 1000µL/min), while pure DMF is injected externally (flow rate = 3000µL/min). The resulting suspension was separated and washed with 3 x 10 mL of DMF.

Solvothermal synthesis: 1 g of CAN(1.8mmol) and 0.6 g of terephthalic acid (3.6 mmol) are mixed in 15 mL of DMF. Pyrex autoclave was closed and placed in an oven heated at 150 °C for 12 hours. Pale yellow crystals were obtained, filtered and washed with 3 x 10 mL of DMF.

2.3 Single Crystal Diffraction‡.

Intensity measurements were carried out at 296K on a Bruker X8 APEX 2 diffractometer equipped with a CCD bidimensional detector using monochromatised Mo-K**α** radiation (λ = 0.71073 Å). An absorption correction was applied using the SADABS program[53] and based on the Blessing method.[54] The structure was solved by direct methods followed by Fourier difference syntheses using the SHELXTL package[55].

As all the first registered crystals have led to very low data quality, our final attempt used a cleaved crystal (0.15*0.1*0.1mm) selected under a polarizing optical microscope and mounted with the viscous oil-drop method. Atoms (except two oxygens and all hydrogen atoms) were anisotropically refined. The H atoms were placed in calculated positions and refined ones by using a riding mode.

High attention has been paid on the verification of the validity of the refinement. All the tests performed on the collected data confirmed the unit cell we used. Either the use of "cell_now" at the beginning of the refinement process (soft for twins and other problem crystals) or the use of "TwinRotMat" (Platon - A Multipurpose Crystallographic Tool) at the end of the data processing did not allow us to determine any twin. All those tests have confirmed the relevance of our refinement. The average reliability factors can be explained mainly by our difficulties to obtain high quality monocristals from solvothermal methods, despite numerous attempts.

Crystallographic data for the $Ce_5(BDC)_{7.5}(DMF)_4$ structure have been deposited at the Cambridge Crystallographic Data Centre (CCDC) as supplementary publication No. 912350.

3. Results and discussions

3.1 One structure from two processes

The cerium-terephthalate MOF nanostructures were synthesized in liquid DMF at 250°C, 10MPa in a coflow reactor (Fig. 1). The operating conditions were controlled with an oil bath (T), a back pressure regulator (p) placed downstream the reactor zone, and two high pressure pumps (flow rates), with the residence time being fixed at 30 seconds. The precursor solution (Cerium Ammonium Nitrate - CAN - and terephthalic acid in DMF) was injected in an inner flow surrounded by a pure DMF outer flow. Coaxial flows are suitable for generating continuously nanostructures, allowing homogenous nucleation in the inner fluid, therefore preventing any clogging problem inherent to heterogeneous nucleation/growth processes on the reactor walls, as previously demonstrated.[56, 57]

Meanwhile, a similar synthesis in DMF was conducted using a standard batch solvothermal process in a Pyrex autoclave at 150°C for 12 hours.

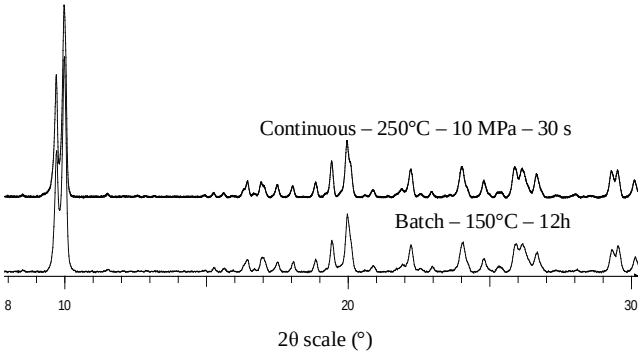

Fig. 2: XRD patterns of the as-synthesized Cerium-based MOF obtained through the batch solvothermal or the continuous HT/HP process.

Both processes lead to pale yellow crystalline powders displaying the same and unique crystalline hybrid phase, which was confirmed by XRD patterns (Fig. 2). Given the very different heating regimes and thus the large kinetics variation between the two processes, the obtained phase can be assumed to be the thermodynamically stable one for the cerium-terephthalate system. It is worth noticing that despite the extremely short residence times employed in the continuous HT/HP process (compared to conventional solvothermal synthesis), the cristallinity of the particles was remarkably great as the diffraction peaks were similar to those obtained with classic solvothermal heating (Fig. 2).

Since the continuous HT/HP process favors nucleation over growth and so the formation of nanostructures, we used the batch solvothermal conditions to promote the growth of the particles and resolve the structure from mono crystal XRay diffraction. Through the synthesis in DMF at 150°C for 3 days, pale yellow crystals have been isolated and were used for XRD structure resolution (see experimental section). The hybrid structure crystallizes in a triclinic structure with general formula: $Ce_5(OOC\text{-}C_6H_4\text{-}COO)_{7.5}(C_3H_7NO)_4$ or $Ce_5(BDC)_{7.5}(DMF)_4$ described afterwards.

3.2 Structure description

The $Ce_5(BDC)_{7.5}(DMF)_4$ structure displays limited cerium chains, all aligned in the same direction, which are linked together through terephthalate ligands. This structure exhibits an arrangement of cerium atoms forming a new Secondary Building Unit (SBU), and a new type of connectivity with other SBUs *via* the terephthalate ligands.

The inorganic SBU are composed of 5 non equivalent crystallographic cerium atoms, arranged linearly (Fig. 3), capped by bridging or chelate bridging terephthalate and DMF molecules. The 7.5 terrephtalic ligands of the SBU can be described as 4 full BDC ligands and 7 half BDC ligands (3.5 BDC) lying about inversion centers. There is neither pure oxo-bridge nor terminal oxygen atom, as it is often the case for lanthanides, meaning that the cerium coordination sphere is composed only of the oxygen atoms from the terephthalate ligands or from the DMF solvent. Cerium atoms located at the extremities of the chains are coordinated to 8 oxygen atoms (2 from DMF molecules, 6 from the terephthalate ligands). The three central cerium atoms are 9 fold-coordinated, from carboxylates ligands.

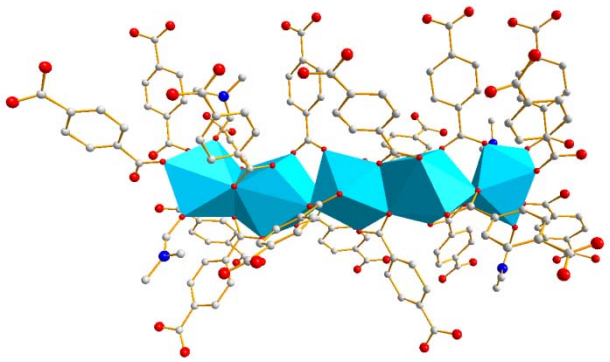

Fig. 3: Ce_5 chains, surrounded by 18 terephtalate ligands and 4 DMF molecules. CeOx polyhedral are represented in cyan, oxygen atoms in red, nitrogen in dark blue and carbon in light gray. Hydrogen atoms are omitted for clarity purposes.

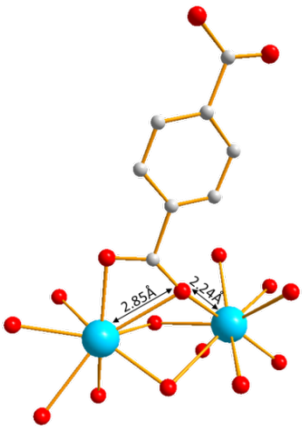

Figure 4: Ball and stick representation of two central cerium atoms of a Ce_5 chain and distances Ce-O displayed by the oxygen atom of a bridging chelate terephthalate ligand between cerium atoms. Hydrogen are omitted for clarity purpose).

Ce-O bonds exhibit various distances (from 2.18(1) Å to 2.88(2) Å) which are consistent to iono-covalent bonding between cerium (8, 9 or 10-coordinated) and carboxylates in the literature.[58-61] The longest Ce-O distances (around 2.8Å) concern oxygen atoms from chelate bridging ligands. The same oxygen atoms are also involved in some of the shortest (and thus stronger) links (Fig. 4). DMF molecules complete the coordination of the ending chain cerium with Ce-O distances (from 2.44(1) to 2.52(2)) indicating a relatively strong and necessary bond for the structure's stability.

Each cerium chain, surrounded by 18 terephthalate ligands and 4 DMF molecules, is connected with 14 other cerium chains: 2 in the same direction, forming hybrid lines, and 12 on the side with close to 60° angle when projected along the 1 -1 0 direction (see Fig. 5). Nitrogen adsorption experiments were performed to evaluate the accessibility of the monodimensionnal triangular channels parallel to the 1 -1 0 axis and proved that are not accessible as the specific area is very low (S_{BET} = 10 m²/g).

Chains located on the same line are connected together via three carboxylate functions, meaning the gap between chains along this direction is very small (Fig. 6). Indeed, measured Ce-Ce distance between 2 chains along this direction is quite closed from Ce-Ce distances inside the same chain ($Ce\text{-}Ce_{inter}$ = 4.764(1) Å and $Ce\text{-}Ce_{intra}$ from 4.013(1) to 4.294(2)Å).

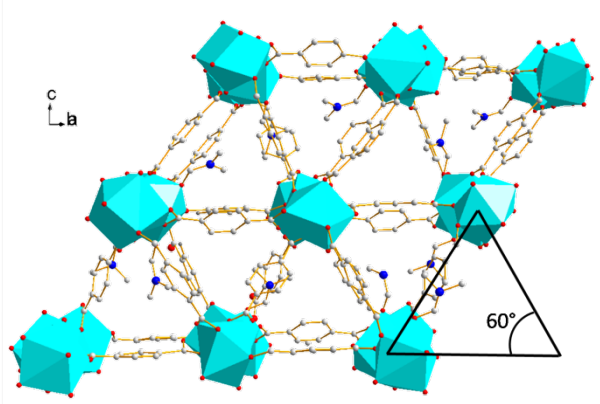

Fig. 5: View of the $Ce_5(OOC\text{-}C_6H_4\text{-}COO)_{7.5}(DMF)_4$ structure along the 1 -1 0 direction.

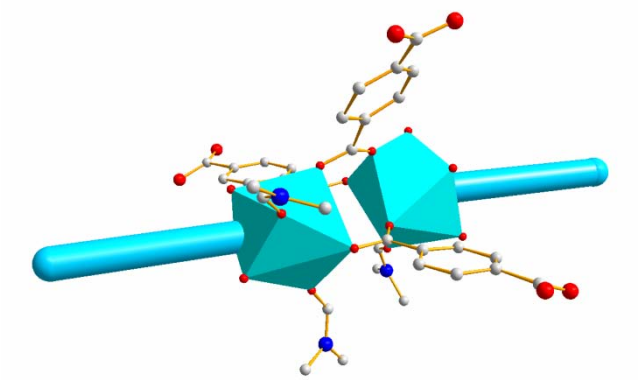

Fig. 6: Extremities of two aligned Ce_5 chains connected via three terephthalate ligands.

3.3. Wide changes in kinetics: the issue of the process

$Ce_5(BDC)_{7.5}(DMF)_4$ was obtained from two different processes involving very different heating regimes and thus different kinetics and reaction pathways: conventional batch solvothermal (150°C, 12 hours) and continuous HT/HP (250°C, 10MPa, 30 s).The main experimental setups and results are summarized table 1 .

The continuous HT/HP synthesis leads flower-shaped ~500 nm MOF nanostructured particles composed of around 100nm crystallites, from TEM characterizations (Fig. 7a). Similarly, SEM analyses show that the batch solvothermal synthesis displayed equivalent morphologies with larger sizes of ~ 15 µm, composed of close to 5 µm sized crystallite (Fig. 7b).

The conventional batch mild temperature solvothermal synthesis (150°C) leads to the crystallization of $Ce_5(BDC)_{7.5}(DMF)_4$ within about 12 hours. Two hours are needed to make the first precipitate appear but XRD patterns show a multiphasic powder for residence times up to 6 hours (see Fig. 8). SEM pictures from 2 and 6 hours powders present crystallites with different morphologies, confirming the presence of at least 2 phases (see ESI-1).

In comparison, the continuous HT/HP process (250°C, 10 MPa) allows for a significant increase in kinetics, resulting in: (i) the obtaining of much smaller particle sizes and (ii) the formation of the $Ce_5(BDC)_{7.5}(DMF)_4$ phase in a shorter residence time.

This can be explained by the higher operating temperature resulting in a higher nucleation (from the general nucleation theory). This effect generates in short time a large number of nuclei, which leave a low concentration of unreacted reagents available for further growth. In comparison, batch mild temperature solvothermal process promotes growth over nucleation, resulting in larger particles. Therefore, we can expect to tailor the particles size by playing with concentration and residence times in the continuous HT/HP process.

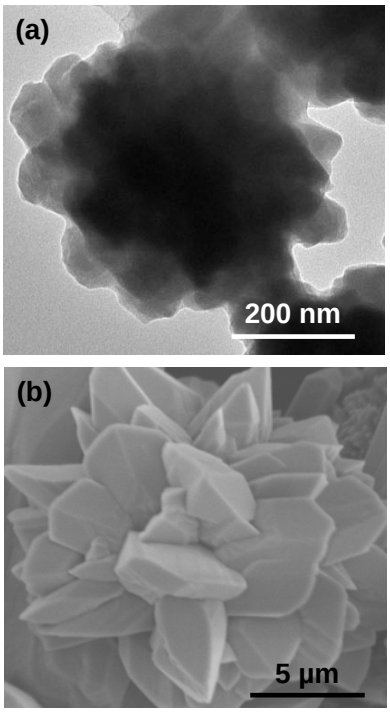

Fig.7: TEM and SEM snap shots of particles of $Ce_5(OOC\text{-}C_6H_4\text{-}COO)_{7.5}(DMF)_4$ obtained from continuous HT/HP process (a) and conventional batch solvothermal process (b), respectively

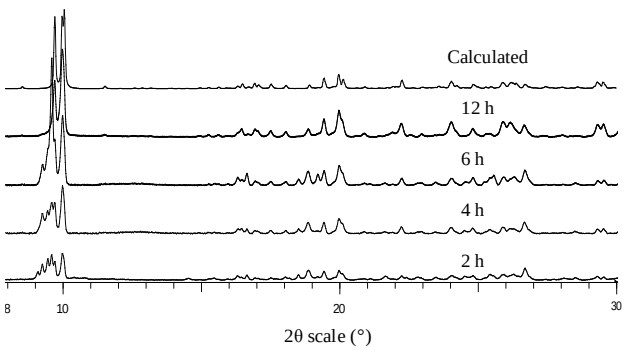

Fig. 8: XRD patterns of samples obtained in solvothermal conditions after different times of synthesis – comparison with the calculated pattern.

Then, considering the new lanthanide-based MOF phase, we can infer that the crystallization of the final hybrid phase is highly promoted by harsh thermodynamic conditions. To confirm this assumption, the temperature of the HT/HP continuous process was decreased to 150°C (similar temperature used in the conventional batch solvothermal synthesis process), all other parameters being kept constant. The resulting sample exhibits a yield that is so low that no powder could even be recovered by centrifugation. However, a TEM grid was prepared by directly casting a drop of the suspension. Pictures are added as ESI-2 and prove the polyphasic aspect of the scarcely visualized particles among which a very small minority of the flower-shaped

Table 1: Main experimental setups and results that allow the comparison between the continuous solvothermal and HT/HP process.

Experimental parameters				Results	
Methods	Temperature (°C)	Time	Pressure (MPa)	Phase(s)	<Ce_5 size> (µm)
Solvothermal	150	12 h	0.1	$Ce_5(BDC)_{7.5}(DMF)_4$	5
Solvothemal	150	6 h	0.1	$Ce_5(BDC)_{7.5}(DMF)_4$, among several phases	5
Solvothermal	150	4 h	0.1	$Ce_5(BDC)_{7.5}(DMF)_4$, among several phases	5
Solvothermal	150	2 h	0.1	$Ce_5(BDC)_{7.5}(DMF)_4$, among several phases	5
HT/HP	250	30s	100	$Ce_5(BDC)_{7.5}(DMF)_4$	0.1
HT/HP	150	30s	100	ε $Ce_5(BDC)_{7.5}(DMF)_4$, among several phases – no powder	0.1
HT/HP	250	30s	25	$Ce_5(BDC)_{7.5}(DMF)_4$	0.1

$Ce_5(BDC)_{7.5}(DMF)_4$. Both low yield and the multiphasic aspect suggest that 150°C is not appropriate for HT/HP process. For short residence times in continuous HT/HP process, temperature appears as a relevant parameter for the yield and the nature of the phases obtained.

The influence of pressure was also considered, by running a similar synthesis at 250°C and 25MPa. As expected, no particular changes were noticed neither for the yield, nor for the average size of the particles, given that the synthesis is done in liquid phase in both cases, resulting in a low density variation.

3.4. Chemical and thermal stability

In this study, CAN - a Ce(IV) precursor - was used for all synthesis. The formula of the structure indicates that it is Ce(III)-based. This has been unambiguously confirmed by XPS spectra (See ESI-3). Indeed, reduction of cerium was expected in presence of DMF. This has already been reported in the literature under milder conditions (50°C): the systematic appearance of $Ce_5(BDC)_{7.5}(DMF)_4$ powder with both process showed that the cerium reduction occurs quite quickly; it cannot be prevented, neither by carboxylates presence, cerium complexation by carboxylates nor by the short residence times.

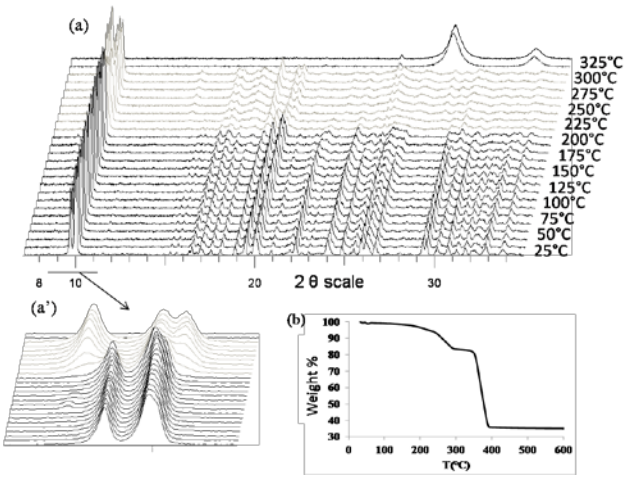

Figure 9:(a) Thermodiffraction experiment in air; two diagrams per 25°C, showing the appearance of an intermediate phase between 200 and 325°C, followed by crystallization of CeO_2; (a') details of the thermodiffraction (9-11°), and (b) Thermal gravimetric analysis of $Ce_5(BDC)_{7.5}(DMF)_4$(5°C/min in air).

Thermal stability of the compound was estimated through thermodiffraction and TGA measurements (see Fig. 9). Thermodiffraction experiment led under air atmosphere shows that the structure evolves from 200°C where a second phase is formed. This phase is stable in situ till 325°C. At this temperature, we observe the decomposition of the MOF and the crystallization of cerium oxide CeO_2. TGA analysis shows that the first consistent loss occurs between 200 and 300°C. It corresponds to DMF molecules (10%$_{exp}$; 11 %$_{theo}$). This leads the Ce_1 and Ce_5 atoms, which are originally in an eightfold coordinated environment with two of the oxygen coordinated from DMF molecules, to a sixfold coordinated environment cerium, which is likely to be a source of unstability (indeed, XRay diffraction on a 200°C overnight heated sample shows that the structure has collapsed). The second important loss is observed at 360°C and stands as the degradation of terephthalic acid molecules (46%$_{exp}$; 49%$_{theo}$).

4. Conclusions

We have reported the synthesis of a new cerium(III)-based metal-organic framework displaying an original topology using a continuous HT/HP (250°C, 10MPa) process. The higher temperature conditions lead to small (~ 500 nm) highly cristalline nanostructured mesoparticles of the thermodynamically-stable $Ce_5(OOC\text{-}C_6H_4\text{-}COO)_{7.5}(DMF)_4$phase in a much short residence time (30 s). In comparison, conventional batch solvothermal synthesis process (150°C) results in the formation of large (~ 10 µm) particles and required 12 hours to form the $Ce_5(OOC\text{-}C_6H_4\text{-}COO)_{7.5}(DMF)_4$ phase. The synthesis pathway towards this crystalline phase is quite robust since the change in thermodynamic conditions does not affect the nature of the crystalline phase obtained.

The structural characterization of the phase was performed through X-Ray diffraction on monocrystals. The compound crystallizes in a triclinic structure displaying limited cerium chains, linked together by terephthalate ligands and stabilized by DMF solvent molecules.

Continuous HT/HP process is extremely efficient to get nanoparticles of highly crystalline hybrid compounds within very short residence times, therefore opening great promises to investigate and synthesize new MOFs nanostructures but also to introduce MOFs in Nanosciences.

Notes and references

[a]*UPMC Univ Paris 06, UMR 7574, Chimie de la Matière Condensée de Paris, Collège de France, 11 place Marcelin Berthelot, 75231 Paris Cedex 05, France. Fax: 33(0)1 44 27 15 04; Tel: 33(0)1 44 27 15 04; E-mail: capucine.sassoye@upmc.fr*

[b]CNRS, UMR 7574, Chimie de la Matière Condensée de Paris, Collège de France, 11 place Marcelin Berthelot, 75231 Paris Cedex 05, France
[c]Collège de France, UMR 7574, Chimie de la Matière Condensée de Paris, Collège de France, 11 place Marcelin Berthelot, 75231 Paris Cedex 05, France
[d]Institut Lavoisier, UMR CNRS 8180, Université de Versailles Saint-Quentin-en-Yvelines, 45 Avenue des Etats-Unis, 78035 Versailles, France
[e]CNRS, Univ. Bordeaux, ICMCB, UPR9048, F-33600 Pessac, France ; Fax: 33(0)5 40 00 27 61; Tel: 33(0)5 40 00 26 72 ; E-mail : aymonier@icmcb-bordeaux.cnrs.fr

†Electronic Supplementary Information (ESI) available: ESI-1: SEM images of two morphologies observed from the powder resulting of batch solvothermal synthesis; ESI- 2 : TEM pictures from grids prepared by directly casting a drop of liquid resulting from HT-HP process at 150°C – 10MPafor a residence time of 30 s. ESI-3: XPS spectra of $Ce_5(OOC\text{-}C_6H_4\text{-}COO)_{7.5}(DMF)_4$ showing the complete absence of Ce(IV).
See DOI: 10.1039/b000000x/

‡$Ce_5O_{34}C_{72}H_{58}N_4$, triclinic, P-1, a=14.105(1)Å, b=15.336(1)Å, c=17.816(1)Å, α=89.985(4)°, β=86.890(4)°, γ=89.747(4)°, V=3848.3(6)Å^3, Z=2, μ=2.991 mm^{-1}, 1.14°<Θ<25.13°, F(000)=2160, 56287 reflections measured at 296K, 12734 independent reflections 10875 Fo > 4σ(Fo). The final reliability factors converged to R_1=0.1599 and wR_2 =0.3720 $I > 2\sigma(I)$, S=1.180; highest residual electron density 3.73e Å^{-3} (all data R_1 =0.1736, wR^2=0.3784).

1. S. T. Meek, J. A. Greathouse and M. D. Allendorf, *Advanced Materials*, 2011, **23**, 249-267.
2. A. U. Czaja, N. Trukhan and U. Muller, *Chemical Society Reviews*, 2009, **38**, 1284-1293.
3. M. Eddaoudi, J. Kim, N. Rosi, D. Vodak, J. Wachter, M. O'Keeffe and O. M. Yaghi, *Science (New York, N.Y.)*, 2002, **295**, 469-472.
4. G. Ferey, C. Mellot-Draznieks, C. Serre, F. Millange, J. Dutour, S. Surble and I. Margiolaki, *Science (New York, N.Y.)*, 2005, **309**, 2040-2042.
5. D. M. Young, U. Geiser, A. J. Schultz and H. H. Wang, *Journal of the American Chemical Society*, 1998, **120**, 1331-1332.
6. J. Lu, T. Paliwala, S. C. Lim, C. Yu, T. Niu and A. J. Jacobson, *Inorganic Chemistry*, 1997, **36**, 923-929.
7. J. Kim, B. Chen, T. M. Reineke, H. Li, M. Eddaoudi, D. B. Moler, M. O'Keeffe and O. M. Yaghi, *Journal of the American Chemical Society*, 2001, **123**, 8239-8247.
8. P. Ayyappan, O. R. Evans and W. Lin, *Inorganic Chemistry*, 2001, **40**, 4627-4632.
9. Z. Wang, C.-M. Jin, T. Shao, Y.-Z. Li, K.-L. Zhang, H.-T. Zhang and X.-Z. You, *Inorganic Chemistry Communications*, 2002, **5**, 642-648.
10. Y. Yoo, Z. Lai and H.-K. Jeong, *Microporous Mesoporous Mater.*, 2009, **123**, 100-106.
11. Z. Wang, K. K. Tanabe and S. M. Cohen, *Chemistry - A European Journal*, 2010, **16**, 212-217.
12. L. Ma, C. Abney and W. Lin, *Chem. Soc. Rev.*, 2009, **38**, 1248-1256.
13. J. Y. Lee, O. K. Farha, J. Roberts, K. A. Scheidt, S. B. T. Nguyen and J. T. Hupp, *Chem. Soc. Rev.*, 2009, **38**, 1450-1459.
14. A. Phan, A. U. Czaja, F. Gandara, C. B. Knobler and O. M. Yaghi, *Inorganic Chemistry*, 2011, **50**, 7388-7390.
15. T. Uemura, D. Hiramatsu, Y. Kubota, M. Takata and S. Kitagawa, *Angewandte Chemie, International Edition*, 2007, **46**, 4987-4990.
16. T. Uemura, T. Kaseda and S. Kitagawa, *Chemistry of Materials.*, 2013, **x**, x-x.
17. E. B. Winston, P. J. Lowell, J. Vacek, J. Chocholousova, J. Michl and J. C. Price, *Physical Chemistry Chemical Physics*, 2008, **10**, 5188-5191.
18. P. Horcajada, C. Serre, M. Vallet-Regi, M. Sebban, F. Taulelle and G. Ferey, *Angewandte Chemie, International Edition*, 2006, **45**, 5974-5978.
19. P. Horcajada, T. Chalati, C. Serre, B. Gillet, C. Sebrie, T. Baati, J. F. Eubank, D. Heurtaux, P. Clayette, C. Kreuz, J.-S. Chang, Y. K. Hwang, V. Marsaud, P.-N. Bories, L. Cynober, S. Gil, G. Ferey, P. Couvreur and R. Gref, *Nature Materials*, 2010, **9**, 172-178.
20. B. Chen, Y. Yang, F. Zapata, G. Lin, G. Qian and E. B. Lobkovsky, *Advanced Materials*, 2007, **19**, 1693-1696.
21. M. Dan-Hardi, C. Serre, T. Frot, L. Rozes, G. Maurin, C. Sanchez and G. Ferey, *Journal of the American Chemical Society*, 2009, **131**, 10857-10859.
22. J. H. Cavka, S. Jakobsen, U. Olsbye, N. Guillou, C. Lamberti, S. Bordiga and K. P. Lillerud, *Journal of the American Chemical Society*, 2008, **130**, 13850-13851.
23. Y. Fu, D. Sun, Y. Chen, R. Huang, Z. Ding, X. Fu and Z. Li, *Angewandte Chemie, International Edition*, 2012, **51**, 3364-3367, S3364/3361-S3364/3325.
24. N. Stock and S. Biswas, *Chemical Reviews*, 2012, **112**, 933-969.
25. S. H. Jhung, J.-H. Lee and J.-S. Chang, *Bulletin of the Korean Chemical Society*, 2005, **26**, 880-881.
26. J. Klinowski, F. A. Almeida Paz, P. Silva and J. Rocha, *Dalton Transactions*, 2011, **40**, 321-330.
27. W.-J. Son, J. Kim, J. Kim and W.-S. Ahn, *Chemical Communications*, 2008, 6336-6338.
28. T. D. Bennett, S. Cao, J. C. Tan, D. A. Keen, E. G. Bithell, P. J. Beldon, T. Friscic and A. K. Cheetham, *Journal of the American Chemical Society*, 2011, **133**, 14546-14549.
29. T. Friscic, D. G. Reid, I. Halasz, R. S. Stein, R. E. Dinnebier and M. J. Duer, *Angewandte Chemie, International Edition*, 2010, **49**, 712-715, S712/711-S712/717.
30. A. L. Garay, A. Pichon and S. L. James, *Chemical Society Reviews*, 2007, **36**, 846-855.
31. A. Demessence, C. Boissiere, D. Grosso, P. Horcajada, C. Serre, G. Ferey, G. J. A. A. Soler-Illia and C. Sanchez, *Journal of Materials Chemistry*, 2011, **20**, 7676-7681.
32. C. Aymonier, A. Loppinet-Serani, H. Reveron, Y. Garrabos and F. Cansell, *Journal of Supercritical Fluids*, 2006, **38**, 242-251.
33. F. Cansell and C. Aymonier, *Journal of Supercritical Fluids*, 2009, **47**, 508-516.
34. S. Moisan, J.-D. Marty, F. Cansell and C. Aymonier, *Chemical Communications*, 2008, 1428-1430.
35. C. Slostowski, S. Marre, O. Babot, T. Toupance and C. Aymonier, *Langmuir*, 2012, **28**, 16656-16663.
36. M. Gimeno-Fabra, A. S. Munn, L. A. Stevens, T. C. Drage, D. M. Grant, R. J. Kashtiban, J. Sloan, E. Lester and R. I. Walton, *Chemical Communications*, 2012, **48**, 10642-10644.
37. A. Carne-Sanchez, I. Imaz, M. Cano-Sarabia and D. Maspoch, *Nature chemistry*, 2013, **5**, 203-211.

38. A. Garcia Marquez, P. Horcajada, D. Grosso, G. Ferey, C. Serre, C. Sanchez and C. Boissiere, *Chemical Communications*, 2013, **49**, 3848-3850.
39. J. Rocha, L. D. Carlos, F. A. A. Paz and D. Ananias, *Chemical Society Reviews*, 2011, **40**, 926-940.
40. Y.-F. Han, X.-Y. Li, L.-Q. Li, C.-L. Ma, Z. Shen, Y. Song and X.-Z. You, *Inorganic Chemistry*, 2010, **49**, 10781-10787.
41. T. M. Reineke, M. Eddaoudi, M. Fehr, D. Kelley and O. M. Yaghi, *Journal of the American Chemical Society*, 1999, **121**, 1651-1657.
42. T. M. Reineke, M. Eddaoudi, M. O'Keeffe and O. M. Yaghi, *Angewandte Chemie, International Edition*, 1999, **38**, 2590-2594.
43. R. D. Shannon, *Acta Crystallographica, Section A: Crystal Physics, Diffraction, Theoretical and General Crystallography*, 1976, **A32**, 751-767.
44. J.-M. Chapuzet, S. Beauchemin, B. Daoust and J. Lessard, *Tetrahedron*, 1996, **52**, 4175-4180.
45. T. Takarada, M. Yashiro and M. Komiyama, *Chemistry - A European Journal*, 2000, **6**, 3906-3913.
46. T. Caruso, E. Bedini, C. De Castro and M. Parrilli, *Tetrahedron*, 2006, **62**, 2350-2356.
47. J. Danan, C. H. De Novion and R. Lallement, *Solid State Communications*, 1969, **7**, 1103-1107.
48. K. Chondroudis and M. G. Kanatzidis, *Inorganic Chemistry Communications*, 1998, **1**, 55-57.
49. J. W. H. van Krevel, J. W. T. van Rutten, H. Mandal, H. T. Hintzen and R. Metselaar, *Journal of Solid State Chemistry*, 2002, **165**, 19-24.
50. W. T. Fu, C. Fouassier and P. Hagenmuller, *Materials Research Bulletin*, 1987, **22**, 389-397.
51. J. Rossat-Mignod, P. Burlet, S. Quezel and O. Vogt, *Physica B*, 1980, **102**, 237-248.
52. O. Guillot-Noel, J. T. M. De Haas, P. Dorenbos, C. W. E. Van Eijk, K. Kramer and H. U. Gudel, *Journal of Luminescence*, 1999, **85**, 21-35.
53. G. M. Sheldrick, *SADABS: A Program for the Siemens Area Detector ABSorption Correction, University of Goettingen, Germany* 1994.
54. R. H. Blessing, *Acta crystallographica. Section A, Foundations of crystallography*, 1995, **51 (Pt 1)**, 33-38.
55. G. M. Sheldrick, *SHELXL, SHELXS: Siemens Analytical X-Ray Instrument, University of Goettingen, Germany.*, 1997.
56. Y. Roig, S. Marre, T. Cardinal and C. Aymonier, *Angewandte Chemie, International Edition*, 2011, **50**, 12071-12074.
57. T. Gendrineau, S. Marre, M. Vaultier, M. Pucheault and C. Aymonier, *Angewandte Chemie, International Edition*, 2012, **51**, 8525-8528.
58. A. Michaelides and S. Skoulika, *Crystal Growth & Design*, 2005, **5**, 529-533.
59. R. Ma, C. Chen, B. Sun, X. Zhao and N. Zhang, *Inorganic Chemistry Communications*, 2011, **14**, 1532-1536.
60. Z.-G. Sun, Y.-P. Ren, L.-S. Long, R.-B. Huang and L.-S. Zheng, *Inorganic Chemistry Communications*, 2002, **5**, 629-632.
61. B.-R. Jian, H.-C. Liu, Y.-W. Lin, S.-C. Huang and K.-F. Hsu, *Microporous Mesoporous Mater.*, 2008, **113**, 187-196.

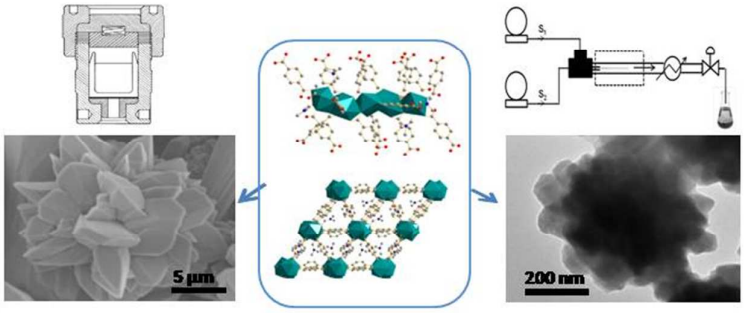

One phase – two processes – two magnitudes for synthesis time and particle size